J Current Pharma Sci. Res., 2024; 1(2):55-65.
https://jcpsr.com

Research Article

Synthesis of Magnetic Nanoparticles Using *Avicennia marina* Leaf Extract and their Potent Antimicrobial and HepG2 Anti-Cancer Activities

Manjula Devi Anandavally Sukumarannair[1], Shilpa Valiyaparambil[2,*]

[1]Department of Pharmacy Practices, Sri Ramakrishna Institute of Paramedical Sciences, College of Pharmacy, Coimbatore, Tamil Nadu, INDIA.
[2]Department of Pharmacy, Annamalai University, Chidambaram, Tamil Nadu, INDIA.

ABSTRACT

Aim: Fabrication of Magnetic Nanoparticles Using *Avicennia marina* Leaf Extract and Assessment of Their Potent Antimicrobial and Anti-Cancer Effects on HepG2 Cells. **Material and Methods:** The study delineates the biosynthesis, characterization, and application of AM-Fe-NPs derived from the aqueous extract of *A. marina* leaves, a coastal plant native to Kozhikode. Phytochemical analysis revealed, such as flavonoids and phenolics, in the *A. marina* leaf aqueous extracts. AM-Fe-NPs were synthesized and characterized by using UV-Visible spectroscopy, FT-IR spectroscopy, Zeta potential and size analysis, EDAX, electron microscopy (FE-SEM and HR-TEM), and XRD. The antibacterial efficacy of the AM-Fe-NPs was evaluated against clinically significant pathogens. Cytotoxic potential of these AM-Fe-NPs was explored on HepG2 cell lines. AM-Fe- NPs success fully synthesised and confirmed nano size by using the characterization techniques. **Results:** AM-Fe-NPs 125 µg/mL showed the significant inhibitory effects against *S. aureus*. Electron microscopic observations further confirmed the antibacterial action, showcasing bacterial cell lysis and shrinking. CLSM studies illustrated a 90% reduction in the *S. aureus* population after nanoparticle treatment. Moreover, the cytotoxic potential of these nanoparticles was explored on HepG2 cell lines, where they exhibited antitumor activity with an IC_{50} value of 31.25 µM. The apoptosis-inducing capability of AM-Fe-NPs in HepG2 cells was visualized using AO/EB fluorescent staining, indicating a significant presence of late-stage apoptotic cells. **Conclusion:** The study underscores the promising biomedical applications of AM-Fe-NPs derived from *A. marina* leaves, demonstrating their potential as antibacterial and anticancer agents.

Keywords: *Avicennia marina*, Aqueous extract, AM-Fe-NPs, Antibacterial activity, Cytotoxicity.

Correspondence:
Mrs. Shilpa Valiyaparambil
Department of Pharmacy, Annamalai University, Chidambaram-608002, Tamil Nadu, INDIA.
Email: shilpavp24@gmail.com

Received: 12-05-2025;
Revised: 21-07-2025;
Accepted: 01-08-2025.

INTRODUCTION

Antibacterial resistance occurs when bacteria adapt in ways that enable them to survive treatments that were once effective against them.[1] This phenomenon has significant complications for both individual patients and public health. Antibiotic inactivity increases irrational use of microbial therapeutic molecules, limiting the treatment options for bacterial infections.[2] Treating infections caused by resistant bacteria is often more difficult, which can result in longer-lasting illnesses and a higher risk of serious complications or even death. Common infections like urinary tract infections and pneumonia may become life-threatening when antibiotics are no longer effective. Additionally, antibiotic resistance can create problems during surgical procedures and cancer treatments, where antibiotics are commonly used to prevent and manage infections. This resistance may lead to complications at surgical sites and delays in necessary treatments. The drug-resistant in bacteria will increase the development of therapeutic microbial drugs, as their effectiveness may be short-lived, posing ongoing challenges in fighting bacterial diseases. To counter these issues, initiatives focus on responsible antibiotic use, the identification of novel antibiotics, and the implementation of robust infection control.[3]

Hepatic (liver) cancer is a malignant disease that starts in the liver, which plays a key role in many essential bodily functions. Cancer that forms in the liver's bile ducts, while less common than Hepatocellular Carcinoma (HCC), can still be aggressive and hard to treat.[4] Persistent hepatitis B or C infection can lead to chronic liver inflammation and significantly increases the risk of liver cancer, as does scarring from long-term alcohol abuse or viral hepatitis.[5]

While liver cancer remains a major health concern, advances in research and treatments offer hope for better patient outcomes. Early detection, timely interventions, routine screenings, and

OPEN ACCESS

Manuscript TECHNOMEDIA

DOI: 10.5530/jcpsr.2024.1.2.9

Publishing Partner : Manuscript Technomedia. [www.mstechnomedia.com]

changes in lifestyle habits are all important strategies for managing and reducing the risk of hepatic cancer.[6] In the present study, AM-Fe-NPs were synthesized using environmentally friendly methods and their antibacterial and anticancer properties were evaluated.

MATERIALS AND METHODS

Avicennia marina collection and extraction

A. marina plant material was carefully gathered from Kozhikode, ensuring the exclusion of any adulterants (Figure 1). Only healthy specimens were chosen, and the collected plants were shade-dried to preserve vital bioactive phytochemicals. The authenticity of the plant sample was verified by Dr. Samuel Tavamani B, an expert in pharmacognosy. Once dried, 500 grams of A. marina leaves were accurately weighed and set aside for further processing. The dried material then underwent cold maceration, a method used to extract valuable bioactive constituents from the plant for subsequent analysis and research.

Synthesis of *A. marina* magnetic nanoparticles (AM-Fe-NPs)

AM-Fe-NPs were prepared using a monohydrated iron nitrate nonahydrate. An aqueous extract of Avicennia marina was mixed and dissolved in distilled water, then rapidly heated to 400°C to initiate the combustion reaction.[7] After the reaction, the product was ground manually, thoroughly rinsed with distilled water, and dried. The resulting AM-Fe-NPs were soaked for two days in a distilled water and 96% ethanol mixture, sonicated, and then coated with a monolayer of *A. marina* extract under basic conditions. The coated nanoparticles were dispersed in distilled water for further study.

Characterization of magnetic AM-Fe-NPs

AM-Fe-NPs were extensively characterized using a variety of advanced analytical techniques. The Bio spec Nano (Shimadzu) instrument was employed to measure the nanoparticles' surface plasmon resonance. ATR-FTIR spectroscopy assessed the functional groups in the extracts responsible for reducing metal salts and facilitating gold and silver nanoparticle formation. For crystalline structure analysis, nanoparticles were mounted on a ZnSe ATR substrate and examined using an X-ray diffractometer (XPERT-PRO). Surface morphology and microscopic features were observed through Field Emission Scanning Electron Microscopy-FE-SEM (TESCAN) and High-resolution transmission electron microscopy-HR-TEM (JEOL Ltd., Japan). Additionally, particle size distribution and zeta potential were determined with the Zetasizer Nano ZS (Malvern Instruments).[8,9]

Culture media and clinical microorganisms

The antimicrobial properties of AM-Fe-NPs were tested against important clinical pathogens. *E. coli, K. pneumoniae*, and *S. aureus* were sourced from the Microbiology Laboratory in Coimbatore, India. Each bacterial strain was individually subcultured in 5 mL of sterile nutrient broth and incubated at optimal conditions (37°C). After incubation, the bacterial suspensions were standardized by adjusting their turbidity to match the MacFarland standard, ensuring consistent cell concentrations for the antimicrobial evaluations.

AM-Fe-NPs antibacterial activity by well plate Method

Antimicrobial properties of AM-Fe-NPs, a well diffusion method was employed. Freshly prepared Mueller Hinton agar (MHA) plates were made using double-strength medium (7.6 g per 100 mL) and sterilized by autoclaving at 121°C for 15 min. Clinical isolates were evenly spread over the surface of the agar using sterile cotton swabs. Sterile borers were then used to create wells in the agar, into which 100 µL of AM-Fe-NPs was carefully dispensed in duplicate, ensuring aseptic conditions throughout the procedure. Tetracycline (10 µg/mL) was used as a control by adding it to separate wells. The plates were placed at 4°C for 30 min to permit the diffusion of the nanoparticles. Following this, they were incubated at 37°C for 24 hr. Zones of inhibition were measured using a HiMedia zone reader.[10]

Determination of Minimal Inhibitory Concentration (MIC) for AM-Fe-NPs

Varying concentrations of AM-Fe-NPs (500, 250, 125, 62.5, 31.25, 15.625, and 7.8125 µg/mL) along with appropriate controls were dispensed into 1.0 mL wells of cell culture plates. Each well then received 100 µL of the test microorganism. The plates were incubated at room temperature for 24 hr. After incubation, the MIC was determined.

FE-SEM and HR-TEM examine antimicrobial effects of AM-Fe-NPs

Bacterial samples treated with AM-Fe-NPs were subjected to centrifugation, washed twice, and then resuspended in Phosphate-Buffered Saline (PBS). The cells were subsequently fixed at room temperature for 2 hr using a 2.5% glutaraldehyde solution. After fixation, the samples were dehydrated in a series of ethanol washes, dried with Hexamethyldisilazane (HMDS), and coated with a thin layer of gold. The structural impact of AM-Fe-NPs on the bacteria was then analyzed using FE-SEM and HR-TEM.

Confocal Laser Scanning Microscopy (CLSM) to examine AM-Fe-NPs treated bacteria

The effect of AM-Fe-NPs on bacterial growth density was evaluated with CLSM. *S. aureus* cultures were grown on coverslips placed in six-well plates, following established protocols. After incubation, the bacterial cells were thoroughly washed with 50 mM Phosphate-Buffered Saline (PBS) at pH 7.4. To preserve

cellular integrity, cells were then fixed in 4% glutaraldehyde at 4°C for 30 min. Bacteria were stained with 0.1% acridine orange for 3 min, then rinsed carefully with PBS to eliminate excess dye. Imaging was performed using a CARL ZEISS LSM 880 confocal microscope (Carl Zeiss, Germany). Quantitative analysis of biofilm density after ortho nitro aniline exposure was conducted using Comstat Software.[11]

Cytotoxicity of AM-Fe-NPs

MTT assay of AM-Fe-NPs

HepG2 cells were seeded into 96-well plates with 100 µL per well, adjusting cell numbers with a hemocytometer and diluting to a density of 1×10^4 cells/mL in DMEM. After incubating for 24 hr at 37°C and 5% CO_2 to facilitate adherence, cells were exposed to various concentrations of AM-Fe-NPs (250 to 1.953 µg/mL) for another 24 hr. Subsequently, the medium was refreshed, and 5 mg/mL MTT in PBS was added. Following 4 hr of incubation, absorbance at 540 nm was recorded with a microplate reader to determine cell viability relative to untreated controls and calculate the IC_{50} value. Each test was performed in duplicate, and inhibition of cell proliferation was determined using the formula:[12]

$$(\text{Control OD} - \text{Test OD}) \times 100$$

AM-Fe-NPs apoptosis study

A staining mixture was made by combining acridine orange and ethidium bromide, each at a final concentration of 100 µg/mL in PBS. HT-29 and HT-116 cells were plated in 96-well plates at 5×10^4 cells per well and incubated for 24 hr. Following exposure to AM-Fe-NPs for 24 hr, cells were detached, rinsed with cold PBS, and stained with the dye mixture at room temperature for 5 min, Stained cells were examined using a fluorescence microscope at 40x magnification, and the proportion of apoptotic cells was calculated out of the total cells in each field.[13]

Statistical analysis

Statistical analysis was carried out using one-way ANOVA to determine differences between the means of three or more groups. All data were processed with GraphPad Prism software version 8.3.0. The findings are reported as the mean ± Standard Deviation (SD) from three separate experiments ($n = 3$).

RESULTS AND DISCUSSION

Plant collection and extraction

Cold maceration is a vital extraction method in pharmacognosy and natural product chemistry. This technique is crucial because it allows for the extraction of bioactive compounds, such as phytochemicals and secondary metabolites, from plant materials at lower temperatures, typically at or near room temperature. By avoiding the application of heat, cold maceration helps preserve the integrity and activity of thermally sensitive compounds, ensuring that the resulting extract retains its medicinal or biological properties. *A. marina* (Figure 1) phytochemicals extracted by the cold maceration method.

Chemical tests-Qualitative aspect

A preliminary analysis was carried out to identify the major phytochemical constituents present in the aqueous leaf extract of *A. marina*. The extract was evaluated for various classes of compounds. The qualitative screening revealed that the aqueous extract contained glycosides, flavonoids, sterols, and proteins or amino acids, while alkaloids, phenolics, carbohydrates, terpenoids, saponins, and tannins were absent. Notably, the detection of flavonoids and glycosides suggests the presence of bioactive molecules known for their antioxidant properties. Overall, the study indicates that the aqueous extract of A. marina leaves is a source of several important phytoconstituents that may contribute to its pharmacological potential.

Synthesis of AM-Fe-NPs

Iron (III) chloride hexahydrate ($FeCl_3 \cdot 6H_2O$) served as the initial substance for producing α-Fe2O3 nanoparticles. The procedure involved gently adding 50 mL of A. marina leaf aqueous extracts to 50 mL of a 0.1M $FeCl_3 \cdot 6H_2O$ solution, maintaining a 1:1 ratio, all at room temperature. Subsequently, 1 M NaOH was introduced until the pH reached 11. The resulting mixture was then agitated using a magnetic stirrer for a duration of 30 min, and the appearance of a highly concentrated black solution confirmed the successful synthesis of iron oxide nanoparticles. These nanoparticles were separated via centrifugation at 8000 rpm for 20 min and thoroughly cleansed through multiple washes with ethanol and water. Finally, the nanoparticles were dried in a hot air oven at 80°C for a period of 3 hr and carefully stored in an airtight container for future utilization.

Figure 1: *A. marina.*

Characterization of AM-Fe-NPs

UV-visible spectroscopy

The AM-Fe-NPs surface plasma resonance was studied using a UV-visible spectrophotometer in the 200-800 nm absorbance range. Figure 3 shows the spectra of the AM-Fe-NPs (Figure 2).

FT-IR spectroscopy

AM-Fe-NPs, FT-IR can be used to analyze the structure and bonding of secondary metabolites on the surface of iron nanoparticles. Iron Peaks related to the iron core would likely be overshadowed by the organic coating, so you might not see much evidence of iron itself in the FT-IR spectrum. *A. marina* secondary metabolites with multiple functional groups, including hydroxyl, carbonyl, and ether groups. -OH Stretching (Around 3200-3600 cm^{-1} for the hydroxyl groups), C=O Stretching (Around 1600-1700 cm^{-1}) for the carbonyl groups and C-O Stretching (Around 1000-1300 cm^{-1}) for the ether and alcohol functionalities. *A. marina* secondary metabolites are chemically bonded or strongly adsorbed to the iron nanoparticles and is coordinated to the iron through one or more of its hydroxyl groups, and the OH stretching peak might shift to a slightly lower wavenumber (Figure 3).

Zeta Size and potential analysis

AM-Fe-NPs are minute particles that exhibit a response to a magnetic field and find extensive applications in biomedicine, catalysis, and various other fields. A key parameter to consider in predicting the stability of colloidal dispersions is the zeta potential, which measures the magnitude of the electrostatic charge repulsion or attraction between particles. For a system to be stable, it typically requires a high absolute value of the zeta potential, often exceeding +30 mV or falling below -30 mV. AM-Fe-NPs zeta potential and size play crucial roles in determining stability, bioavailability, and interactions with biological systems. The zeta potential and size values mentioned for the synthesized nanoparticles, such as AM-Fe-NPs having a zeta potential of -25.9 mV along with their corresponding size values (88.20), are important indicators of their behaviour and potential applications (Figures 4 and 5).

EDAX analysis

EDAX analysis showed the presence of primary element of interest here is Iron (Fe), Carbon (C), Hydrogen (H), Oxygen (O), and possibly Phosphorous (P) and Nitrogen (N) if secondary metabolites (Figure 6).

Electron microscope (FE-SEM and HR-TEM) observation

FE-SEM and HR-TEM confirmed the surface morphology and size of the nanoparticles. Magnetic Fe_3O_4NPs exhibited a uniform and smooth appearance, characterized by oval-shaped liposomes. (Figures 7 and 8).

XRD-AM-Fe-NPs

The crystalline structure of the iron oxide nanoparticles was characterized by XRD analysis. Plant A extract NPs 2Θ= 23.452, 29.591, 41.173, 43.588, 45.291, 55.975, 61.540 and 71.639 show the crystalline nature of the nanoparticles (Figure 9).

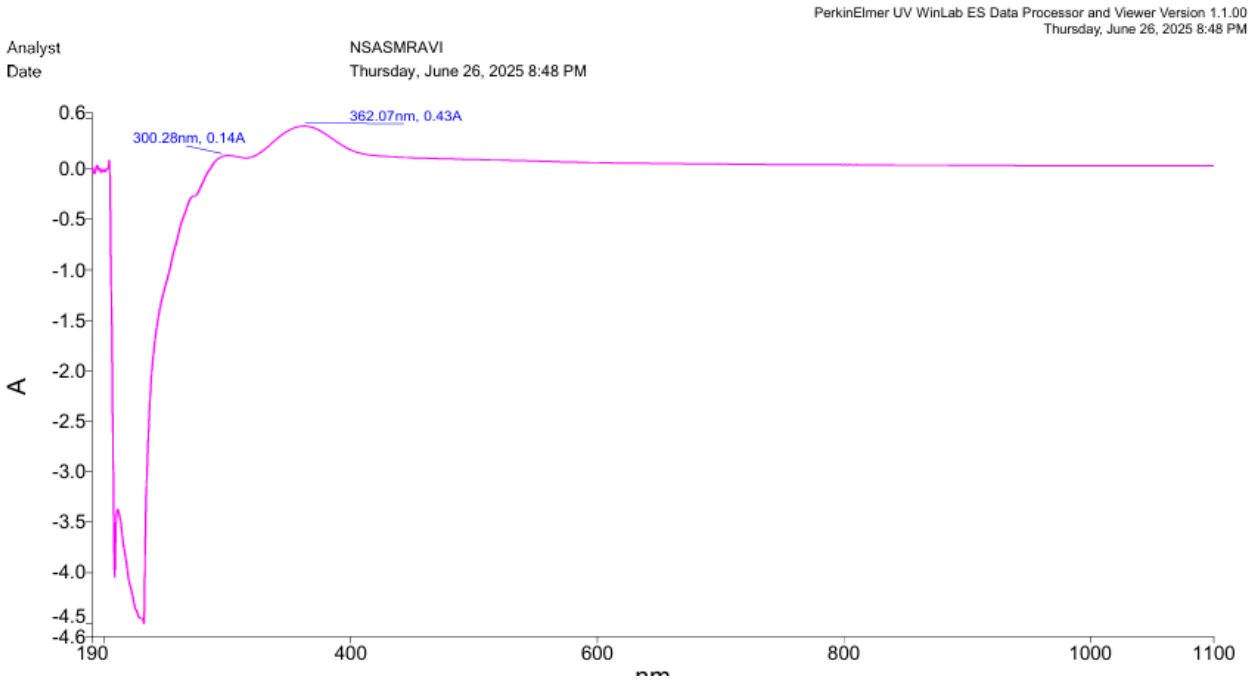

Figure 2: AM-Fe-NPs UV spectroscopy analysis.

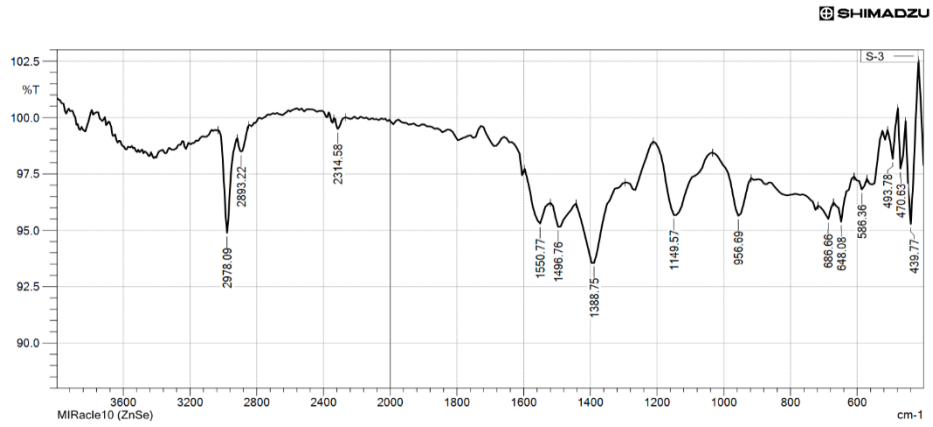

Figure 3: FT-IR spectrum of AM-Fe-NPs

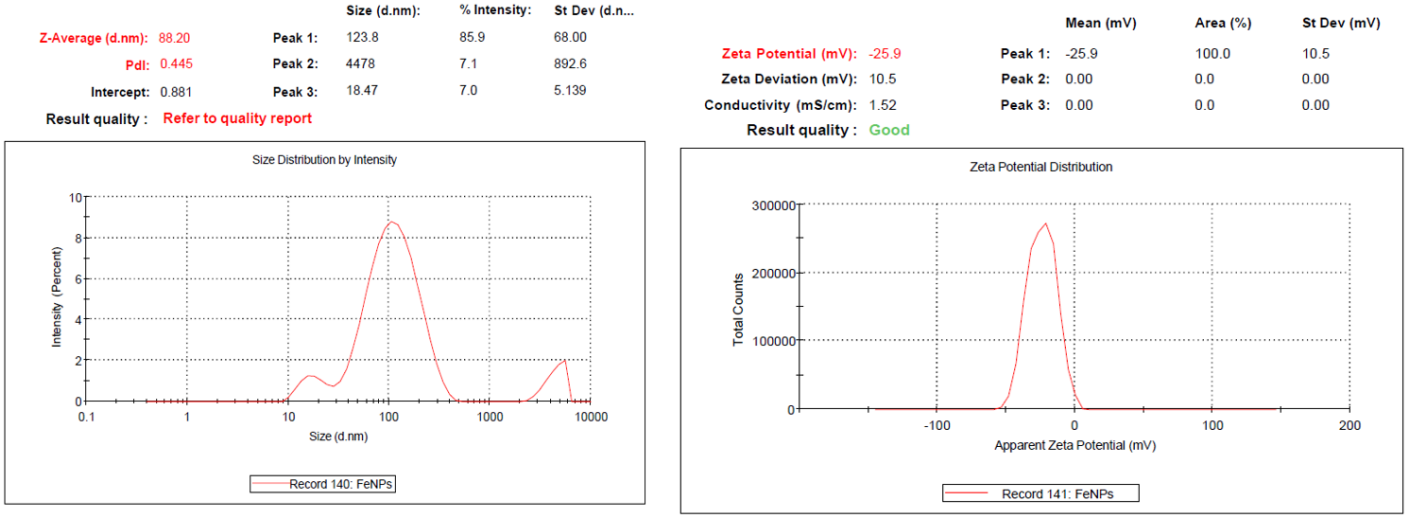

Figure 4: Zeta size and zeta potential of AM-Fe-NPs.

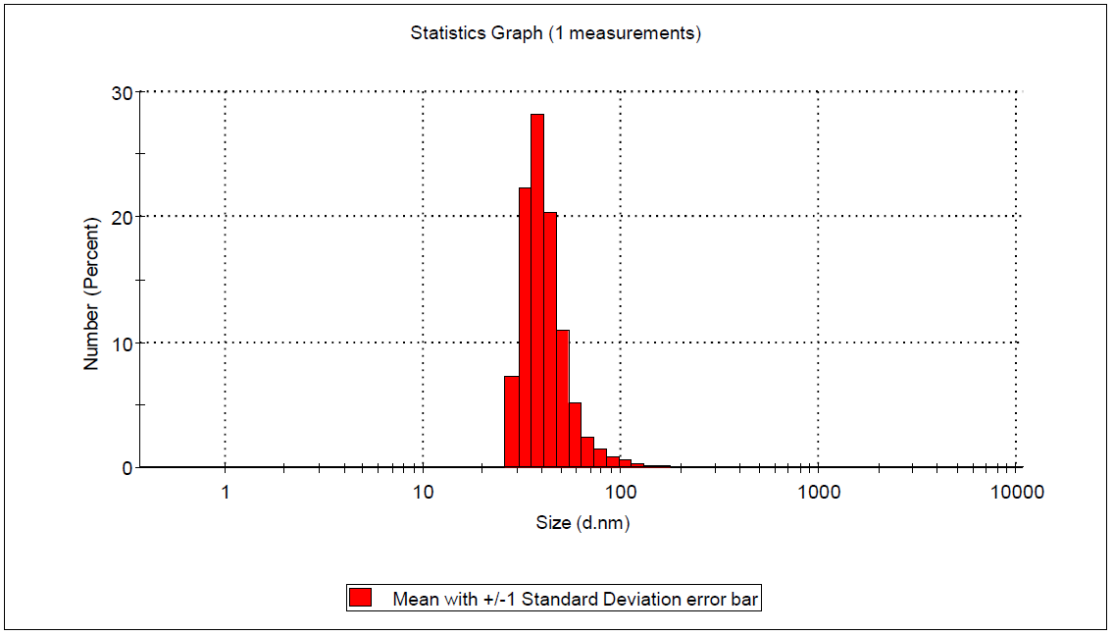

Figure 5: Zeta size distribution of AM-Fe-NPs.

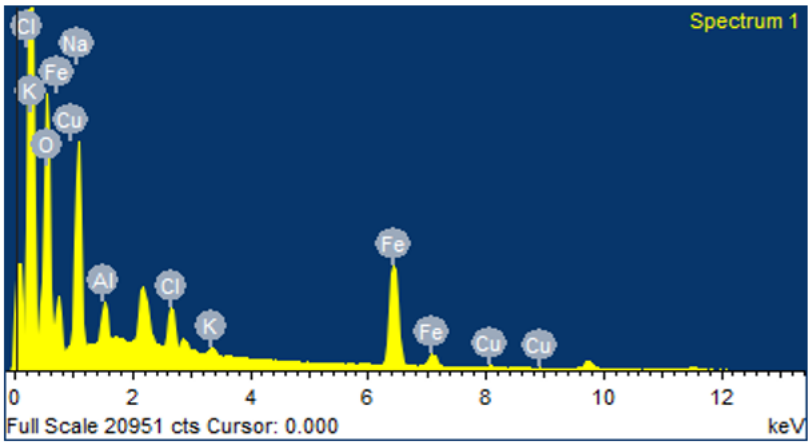

Figure 6: EDAX analysis of AM-Fe-NPs.

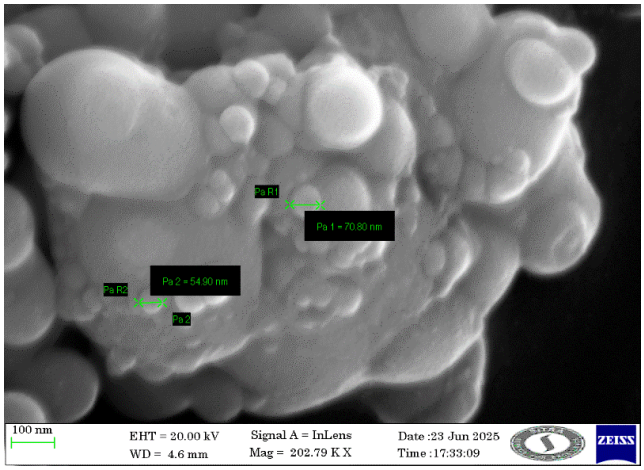

Figure 7: FE-SEM analysis of AM-Fe-NPs.

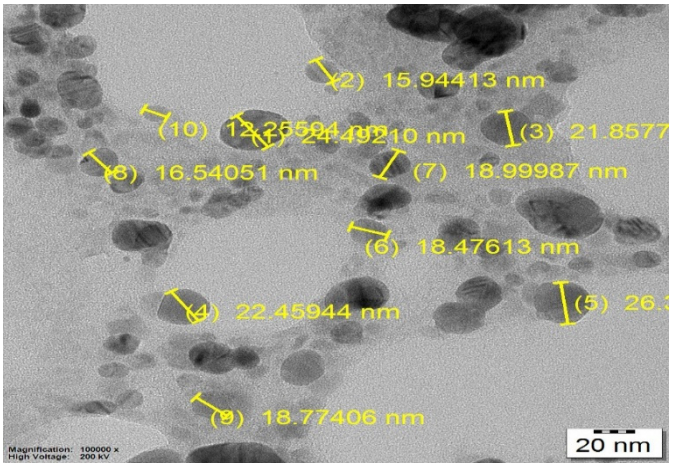

Figure 8: HR-TEM analysis of AM-Fe-NPs.

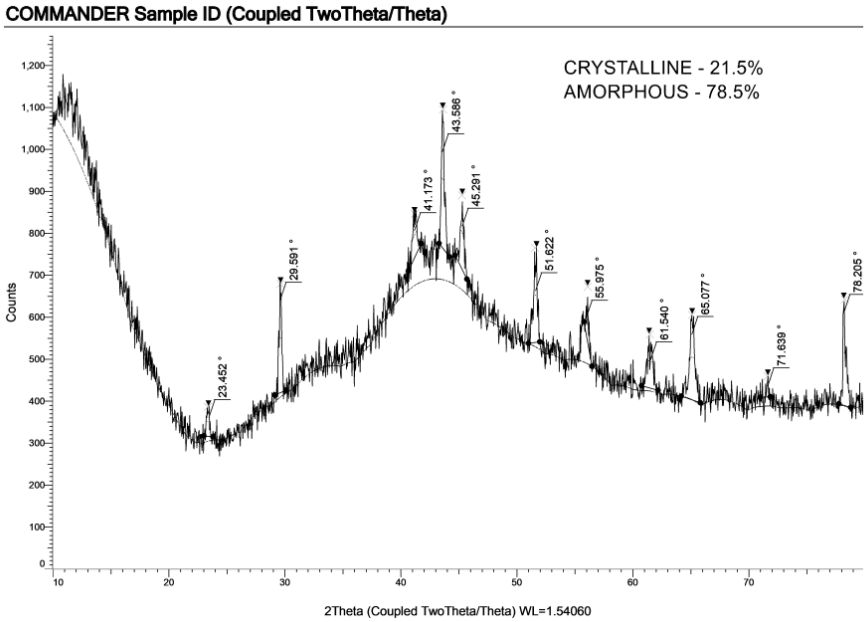

Figure 9: XRD-analysis of AM-Fe-NPs.

Antibacterial activity of AM-Fe-NPs

The agar-well diffusion method was utilized to evaluate the antimicrobial efficacy of AM-Fe-NPs against clinically relevant pathogens. Plates were prepared with a layer of the pertinent clinical microbe. The resulting zones of inhibition were identified by measuring their diameters, and the findings can be viewed in Figure 10.

Figure 10 displays the antibacterial activity of AM-Fe-NPs and ciprofloxacin against several clinical bacterial strains. Among those tested, only *S. aureus* exhibited susceptibility to the AM-Fe-NPs, showing a zone of inhibition of 17 mm, while no inhibitory effect was observed for the other microorganisms listed.

MIC of AM-Fe-NPs

The antimicrobial susceptibility of AM-Fe-NPs against *S. aureus* was evaluated to determine its minimum inhibitory activity. At a concentration of 125 µg/mL, the AM-Fe-NPs exhibited significant inhibitory effects. MIC was ascertained using tetrazolium staining. In the presence of active reductase enzymes from live bacterial cells, the yellow tetrazolium was converted to a red hue. In contrast, dead bacterial cells, lacking the active reductase enzyme, were unable to facilitate this color change. Based on the tetrazolium staining outcomes, it is evident that AM-Fe-NPs effectively curbed *S. aureus* growth at the specified concentration of 125 µg/mL.

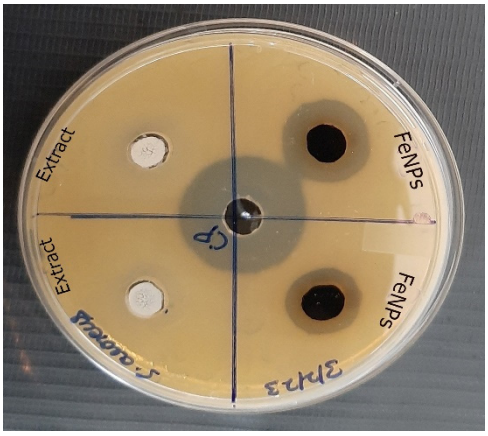

Figure 10: Antimicrobial activity of AM-Fe-NPs and Ciprofloxacin drugs against *S. aureus*.

FE-SEM and HR TEM examination of AM-Fe-NPs treated bacterial cells

The morphology of AM-Fe-NPs treated bacterial cells was observed using an electron microscope. From the electron microscopic observation (FE-SEM and HR TEM), bacterial cell lysis and shrinking confirmed that AM-Fe-NPs (125 µg/mL) inhibited the growth of the clinical bacteria *S. aureus* (Figures 11 and 12).

Bacterial cells treated with 125 µg/mL AM-Fe-NPs were examined using HR-TEM followed by EDAX. The combined HR-TEM-EDAX evaluation verified the presence of Iron (Fe) within the bacterial cells. This evidence supports the assertion that AM-Fe-NPs exhibit antibacterial properties against *S. aureus*.

CLSM to examine antimicrobial effects of AM-Fe-NPs

The bacterial growth observation AM-Fe-NPs treated bacterial cells by using CLSM. From the CLSM observation, bacterial cell growth was reduced as compared to the control (Figure 13).

Using CLSM, an advanced imaging technique that enhances resolution by filtering out-of-focus light in thicker specimens, a quantitative analysis of *S. aureus* treated with AM-Fe-NPs was performed. This technology, employing a specialized pinhole to eliminate extraneous light, allowed for detailed 2D and 3D evaluations. Results indicated a remarkable 90% reduction in

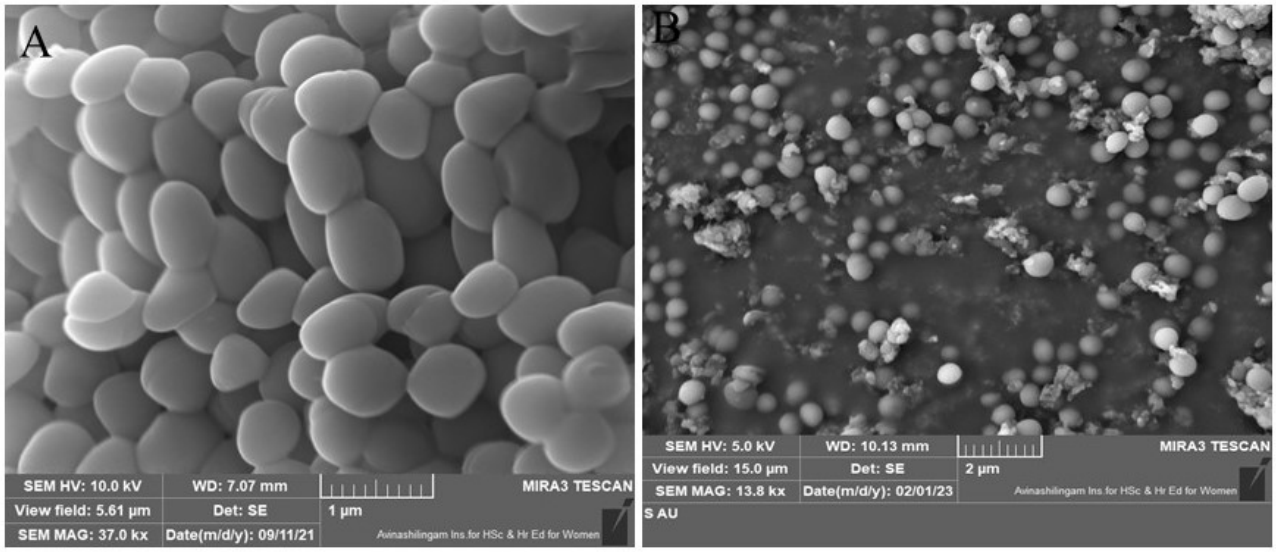

Figure 11: A: FE-SEM observation of *S. aureus*, B: FE-SEM observation of AM-Fe-NPs (Bacterial cell damage).

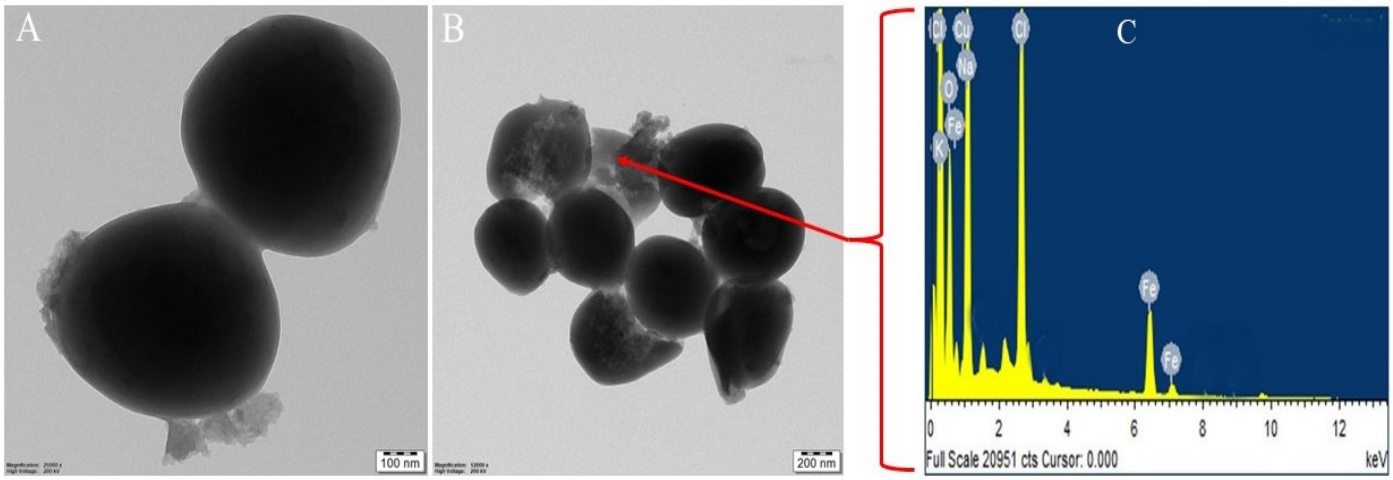

Figure 12: A: HR-TEM observation of *S. aureus*, B: HR-TEM observation of AM-Fe-NPs treated *S. aureus* (Bacterial cell damage).

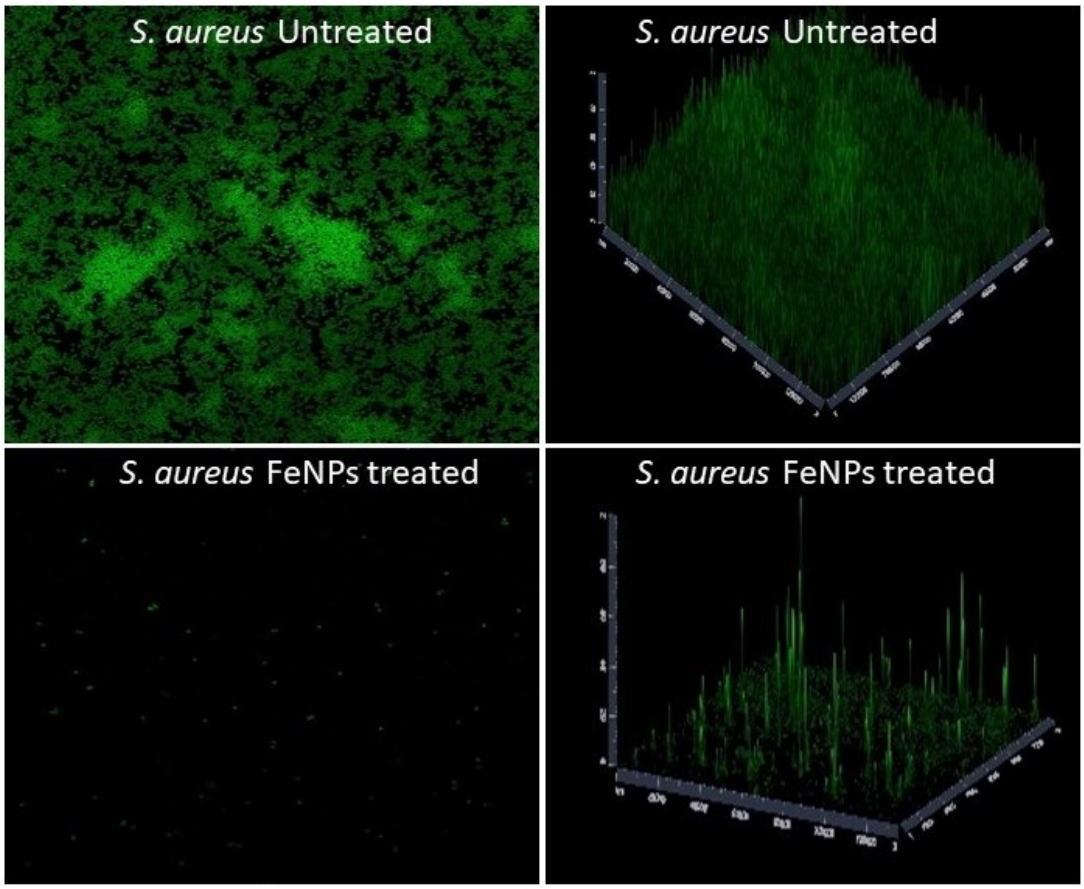

Figure 13: Bacterial growth observation of AM-Fe-NPs treated bacterial cells by using a CLSM.

the *S. aureus* population post-treatment with the nanoparticles compared to the untreated control. This substantial decline suggests that AM-Fe-NPs are effective in inhibiting the growth of the bacteria. To facilitate visualization under CLSM, the microbial cells were stained with acridine orange, producing a distinct green fluorescence. The quantitative data derived from the CLSM are invaluable for determining specific metrics, such as microbial density.

Cytotoxicity of AM-Fe-NPs

MTT Assay of AM-Fe-NPs

The antitumor activity of AM-Fe-NPs was assessed using the MTT assay in HepG2 cell lines. The IC_{50} value, representing the concentration of the complex at which 50% cell destruction occurred, was determined by plotting cell viability against

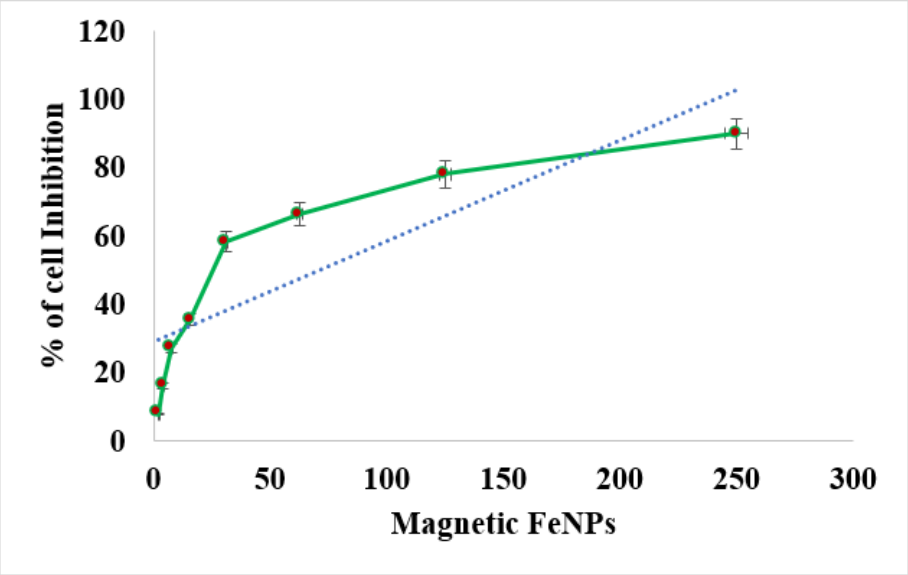

Figure 14: Cytotoxicity of AM-Fe-NPs on cell lines.

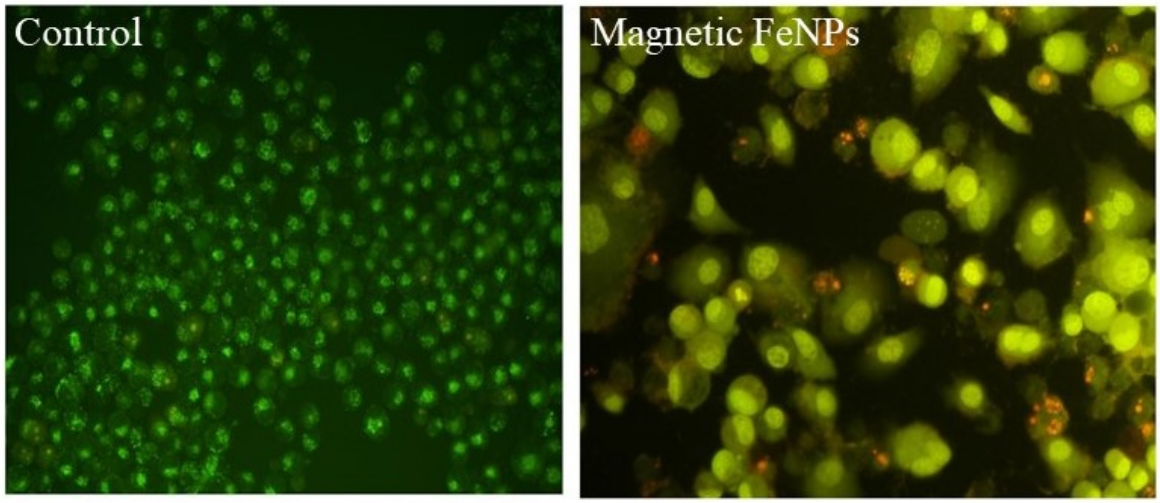

Figure 15: A: HepG2 control cells. B: In HepG2 cells treated with AM-Fe-NPs, late-stage apoptotic cells, characterized by highly condensed or fragmented chromatin, emit fluorescence ranging from shades of orange to red.

AM-Fe-NPs. AM-Fe-NPs, the IC_{50} value against HepG2 cells after 24 hr of exposure was found to be 31.25 µM (Figure 14).

Fluorescent staining for apoptosis

To investigate any morphological changes in HepG2 cells after exposure to AM-Fe-NPs, we utilized AO/EB fluorescence staining, illustrated in Figure 15. This staining technique enabled us to discern the apoptotic characteristics triggered by AM-Fe-NPs within the HepG2 cells.

CONCLUSION

This research has shed light on the multifaceted applications of AM-Fe-NPs synthesized using an aqueous extract of *A. marina* leaves. The green synthesis method presented here offers a sustainable and eco-friendly avenue for nanoparticle production. The obtained Fe_3O_4 nanoparticles demonstrated significant antibacterial activity against *S. aureus* and potential antitumor properties against HepG2 cells. The induction of apoptosis in HepG2 cells treated with AM-Fe-NPs also highlights its potential in cancer therapy. Given these promising results, further investigations on the therapeutic potential of these nanoparticles are warranted, including comprehensive *in vivo* studies and potential scale-up for therapeutic applications

ACKNOWLEDGEMENT

The authors thank the Department of Pharmacy, Annamalai University, for providing the necessary research facilities.

ABBREVIATIONS

AM-Fe-NPs: *A. marina* iron nanoparticles; **UV:** Ultra Violet-Visible spectroscopy; **FT-IR:** Fourier transformed infrared spectroscopy; **EDAX:** Energy dispersive X-ray analysis; **FE-SEM:** Field emission scanning electron microscopy; **HR-TEM:** High-resolution transmission electron microscopy; **CLSM:** Confocal laser scanning microscopy; **HepG2:** Hepatoblastoma cell line; **NCCS:** National Centre for Cell Sciences; **MTT:** 3-(4,5-dimethylthiazol-2-yl)-2,5-diphenyltetrazolium bromide; **PBS:** Phosphate-buffered saline.

CONFLICT OF INTEREST

The authors declare that there is no conflict of interest.

SUMMARY

This research focused on the green synthesis of magnetic iron oxide nanoparticles (AM-Fe-NPs) using an aqueous leaf extract from the mangrove plant Avicennia marina (A. marina). The plant material was carefully collected, and bioactive compounds were extracted through the cold maceration method, which preserves thermally sensitive phytochemicals by operating at room temperature without heat application. This extraction process ensured the retention of key secondary metabolites with potential biological activity. Initial qualitative chemical tests on the A. marina extract revealed the presence of glycosides, flavonoids, sterols, and proteins or amino acids, while other common phytochemical groups such as alkaloids, phenolics, terpenoids, saponins, tannins, and carbohydrates were absent. The flavonoids and glycosides identified in the extract may underlie the extract's pharmacological potential, especially its antioxidant properties. For the synthesis of iron oxide nanoparticles, an equal ratio of the A. marina aqueous leaf extract was mixed with an iron precursor (FeCl3·6H2O) at room temperature, followed by pH adjustment and stirring. The formation of a concentrated black solution signaled successful nanoparticle synthesis. The nanoparticles were then separated, thoroughly washed, dried, and stored for further use. Characterization of the AM-Fe-NPs involved several sophisticated techniques. UV-visible spectroscopy confirmed the distinctive surface plasmon resonance specific to nanoparticles. FT-IR spectroscopy showed key signatures of secondary metabolites on the nanoparticles' surface, indicating successful functionalization with plant-derived molecules particularly with functional groups like hydroxyl, carbonyl, and ether. Zeta potential and size analyses revealed that the AM-Fe-NPs had a zeta potential of -25.9 mV and an average size of 88.2 nm, signifying moderate colloidal stability an important factor for their biological interactions and application potential. Elemental analysis (EDAX) confirmed the presence of iron, carbon, oxygen, and other trace elements associated with the plant's secondary metabolites. Morphological studies using electron microscopy (FE-SEM and HR-TEM) showed that the nanoparticles possessed a uniform, smooth, and oval structure. Additionally, X-ray diffraction (XRD) confirmed the crystalline nature of the synthesized iron oxide nanoparticles. The synthesized nanoparticles were evaluated for their antimicrobial activity using the agar-well diffusion method. The results showed that the AM-Fe-NPs were particularly effective against Staphylococcus aureus (S. aureus), exhibiting a significant zone of inhibition, while other bacteria were less affected. Minimum inhibitory concentration (MIC) testing revealed that S. aureus growth was substantially inhibited at a concentration of 125 µg/ml. Further electron microscopic examination of treated bacterial cells confirmed bacterial cell damage and lysis, and elemental analysis demonstrated that iron was effectively delivered into the bacterial cells. In addition to antibacterial activity, the cytotoxic effects of AM-Fe-NPs were assessed on HepG2 liver cancer cell lines. Using the MTT assay, the IC50 the concentration that killed half of the tumor cells was determined to be 31.25 µM after 24 hours, indicating strong antiproliferative activity. Fluorescent staining further showed that AM-Fe-NPs induced apoptotic changes in these cancer cells, hinting at a potential mechanism for their antitumor action. In conclusion, this work demonstrates that iron oxide nanoparticles synthesized via a green, plant-based method possess promising antimicrobial and anticancer properties. The use of A. marina leaf extract not only provides an eco-friendly nanoparticle synthesis approach but also enhances the biological potential of the nanoparticles. These findings lay the groundwork for future studies to explore their therapeutic applications, including further in vivo research and potential development for clinical use

REFERENCES

1. Prasad S, V P S, Abbas HS, Kotakonda M. Mechanisms of antimicrobial resistance: highlights on current advance methods for detection of drug resistance and current pipeline antitubercular agents. Curr Pharm Biotechnol. 2022; 23(15): 1824-36. doi: 10.2174/1389201023666220318104042, PMID 35306984.
2. Ventola CL. The antibiotic resistance crisis: Part 1: Causes and threats. P T. 2015; 40(4): 277-83. PMID 25859123.
3. Llor C, Bjerrum L. Antimicrobial resistance: risk associated with antibiotic overuse and initiatives to reduce the problem. Ther Adv Drug Saf. 2014; 5(6): 229-41. doi: 10.1177/2042098614554919, PMID 25436105.
4. Testino G, Borro P. Chemoprevention of hepatocellular carcinoma in patients with hepatitis C virus related cirrhosis. World J Hepatol. 2013; 5(10): 521-7. doi: 10.4254/wjh.v5.i10.521, PMID 24179611.
5. Chidambaranathan-Reghupaty S, Fisher PB, Sarkar D. Hepatocellular carcinoma (HCC): epidemiology, etiology and molecular classification. Adv Cancer Res. 2021; 149: 1-61. doi: 10.1016/bs.acr.2020.10.001, PMID 33579421.
6. Marengo A, Rosso C, Bugianesi E. Liver cancer: connections with obesity, fatty liver, and cirrhosis. Annu Rev Med. 2016; 67: 103-17. doi: 10.1146/annurev-med-090514-013832, PMID 26473416.
7. Wu W, He Q, Jiang C. Magnetic iron oxide nanoparticles: synthesis and surface functionalization strategies. Nanoscale Res Lett. 2008; 3(11): 397-415. doi: 10.1007/s11671-008-9174-9, PMID 21749733.
8. Ali A, Zafar H, Zia M, Ul Haq I, Phull AR, Ali JS, *et al.* Synthesis, characterization, applications, and challenges of iron oxide nanoparticles. Nanotechnol Sci Appl. 2016; 9: 49-67. doi: 10.2147/NSA.S99986, PMID 27578966.
9. Abbas HS, Krishnan A, Kotakonda M. Fabrication of Iron oxide/zinc oxide nanocomposite Using Creeper *Blepharis maderaspatensis* Extract and Their antimicrobial Activity. Front Bioeng Biotechnol. 2020; 8: 595161. doi: 10.3389/fbioe.2020.595161, PMID 33392168.

10. Kotakonda M, Marappan M, Dharmar P, Sakthivel B, Sunnapu P. Isolation and identification of bioactive compounds with antimicrobial activity from marine facultative anaerobe, *Bacillus subtilis*. Curr Pharm Biotechnol. 2023; 24(5): 698-707. doi: 10.2174/1389201023666220801090810, PMID 35927910.
11. Alovisi M, Pasqualini D, Mandras N, Roana J, Costamagna P, Comba A, *et al.* Confocal laser scanner evaluation of bactericidal effect of chitosan nanodroplets loaded with benzalkonium chloride. J Clin Med. 2022; 11(6): 1650. doi: 10.3390/jcm11061650, PMID 35329976.
12. Satyavani K, Gurudeeban S, Ramanathan T, Balasubramanian T. Toxicity Study of Silver Nanoparticles Synthesized from *Suaeda monoica* on Hep-2 Cell Line. Avicenna J Med Biotechnol. 2012; 4(1): 35-9. doi: 10.18502/ajmb.v17i2.18567, PMID 23407847.
13. Kari S, Subramanian K, Altomonte IA, Murugesan A, Yli-Harja O, Kandhavelu M. Programmed cell death detection methods: a systematic review and a categorical comparison. Apoptosis. 2022; 27(7-8): 482-508. doi: 10.1007/s10495-022-01735-y, PMID 35713779.